Formation and decomposition of Si hydrides during adsorption of Si_2H_6 onto Si(100)(2×1)

Masanori Shinohara, Akio Seyama, Yasuo Kimura, and Michio Niwano*
Research Institute of Electrical Communication, Tohoku University, 2-1-1 Katahira, Aoba-ku, Sendai 980-8577, Japan

Mineo Saito
NEC Informatec Systems, Ltd., 34 Miyukigaoka, Tsukuba 305-8501, Japan
(Received 4 September 2001; published 1 February 2002)

Infrared absorption spectroscopy in the multiple internal reflection geometry and hybrid density-functional cluster calculation are used to characterize the adsorption structure of hydride species that form during adsorption of disilane on Si(100)(2×1) at room temperature. We suggest that disilane dissociatively adsorbs without breaking its Si—Si bond to produce an adatom dimer, —H_2Si—SiH_2—, that bridges two adjacent dimers. We demonstrate that at low hydride coverage, a trihydride (—SiH_3) formed by breaking the Si—Si bond of Si_2H_6, decomposes into dihydride and monohydrides, while at high hydride coverage, the trihydride decomposition is quenched. We also suggest that the impinging rate of adsorbing molecules has a significant effect on the adsorption kinetics.

DOI: 10.1103/PhysRevB.65.075319 PACS number(s): 82.65.+r, 68.43.−h, 82.80.Dx

I. INTRODUCTION

Adsorption of disilane, Si_2H_6, onto Si(100) has so far been investigated extensively, because of the potential of using disilane as the source gas for gas source molecular-beam epitaxy (GS-MBE) for the growth of Si. It has been demonstrated that Si(100) growth rate is enhanced using Si_2H_6, rather than the conventional SiH_4 gas, due to higher adsorption rates associated with the ease of cleaving Si—Si bonds, compared to Si—H bonds.[1,2] The growth kinetics of Si GS-MBE epitaxy from Si_2H_6 was well described by models based upon second-order adsorption and first-order hydrogen desorption kinetics.[1–3] Previous studies on Si deposition using Si_2H_6 (Refs. 4–9) have shown that at temperatures above 700 K and fractional surface hydrogen coverage less than one monolayer, Si_2H_6 dissociatively adsorbs on Si surface dangling bonds as two trihydride (SiH_3) species which subsequently decompose to surface monohydride, SiH. Then, how does disilane adsorb onto Si surfaces at lower surface temperatures? Elucidating the adsorption process of disilane at a wider range of substrate temperature is beneficial to the fundamental understanding and the atomic level controlling of Si crystal growth using Si_2H_6. Previously, detailed atom-resolved studies using the scanning tunneling microscope (STM) have demonstrated that at room temperature, disilane dissociates to produce dihydride species (—SiH_2) and two monohydride species.[10] However, it seems unlikely that at room temperature disilane completely dissociates into monohydride and dihydride species. It would be rather be likely that a variety of intermediate surface species, which eventually decompose to monohydride and dihydride species, are populated during the course of disilane adsorption.

In this study, we have investigated the adsorption of Si_2H_6 on the Si(100)(2×1) surface using infrared absorption spectroscopy (IRAS) in the multiple internal reflection geometry (MIR) (Ref. 11) and the so-called hybrid density-functional theory (DFT). IRAS-MIR provides us with valuable information about the hydrogen bonding configurations on semiconductor surfaces.[12,13] We analyze IRAS spectra in the Si-H stretching vibration region to determine the type of hydride species that are populated upon Si_2H_6 adsorption. Comparison of experimental data with results of DFT calculation leads to clear identification of the observed peaks due to surface hydride species, as has been previously demonstrated by Weldon *et al.* on the H_2O oxidation of Si(100)×(2×1).[14] As a result, we found interesting adsorption processes: disilane misses two hydrogen atoms and bridges the two adjacent surface dimers. This process occurs *without breaking the* Si—Si *bond of disilane*. When the Si—Si bond of disilane is broken, two surface silyl (—SiH_3) groups are produced that further decompose into monohydrides. We found that at high hydride coverage, the decomposition of trihydride is quenched. These findings would give important insight into the microscopic mechanism of Si crystal growth in GS-MBE using disilane.

II. EXPERIMENTAL PROCEDURES

Samples used here were obtained from *n*-type *P*-doped Si(100) wafers with resistivities of approximately 10 Ω cm. Samples were introduced into an ultrahigh-vacuum (UHV) chamber, the base pressure of which was low in the range of 10^{-10} Torr. The sample surface was cleaned by resistively heating up to about 1200 K. After surface cleaning, the surface was exposed to Si_2H_6. The Si_2H_6 exposures are given in langmuir (1 L = 10^{-6} Torr s), as determined by the product of the partial pressure of molecular disilane, and time. The dosing pressure of Si_2H_6 was in the range of 10^{-9}–10^{-7} Torr. As mentioned below, we observed that the surface exposed to Si_2H_6 at different dosing pressures but with the same amount of exposure exhibit quite different spectral shapes. This suggests that the impinging rate of adsorbing molecules may have a significant influence on the adsorbing kinetics. This point will be discussed later. The chemical state of the Si_2H_6-adsorbed Si(100) surface was

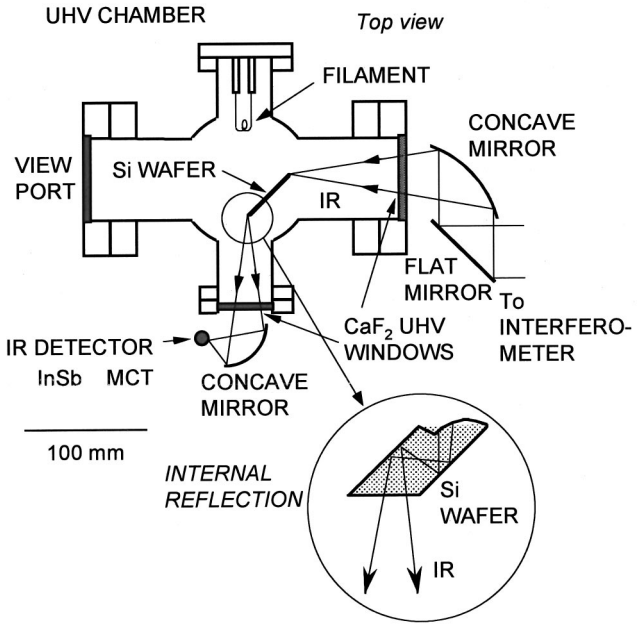

FIG. 1. Experimental setup for IRAS measurements.

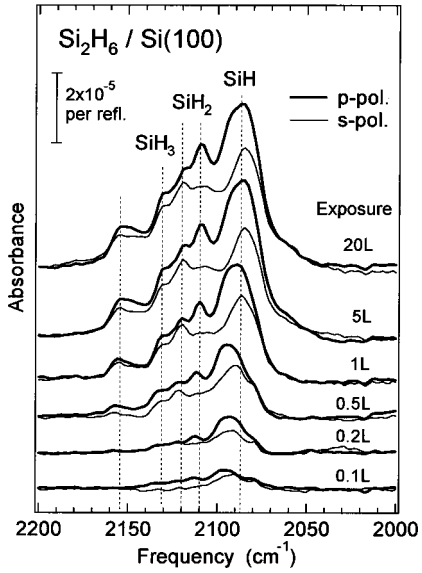

FIG. 2. Si-H stretching vibration spectra of the Si(100) surface exposed to Si_2H_6 for different exposures at room temperature.

monitored by MIR-IRAS. The experimental setup was the same as used in our previous works.[15–17] Samples used for the MIR-IRAS measurements were $0.5\times10\times40\ mm^3$ with 45° bevels on each of the short edges. The infrared radiation that exited an interferometer (BOMEM MB-100) was focused at normal incidence onto one of the two bevels of the sample, and penetrated through the wafer, internally reflecting about 80 times, as is schematically illustrated in Fig. 1. The radiation that exited the sample at the other bevel was focused onto a liquid-N_2-cooled HgCdTe (MCT) detector. The reference spectrum was recorded after surface cleaning. The resolution of the interferometer was set at 4 cm^{-1}, which is adequate for determining the type of Si hydride species.

III. RESULTS AND DISCUSSION

A. Si-H vibration spectra

Figure 2 shows *p*- and *s*-polarized IRAS spectra in the Si-H stretching vibration region of the Si(100)(2×1) surface that was exposed to disilane at room temperature (RT). In the figure, we plot a series of spectra that have been obtained by increasing step by step the disilane exposure up to 20 L at a dosing pressure of 10^{-9}–10^{-8} Torr. Some absorption peaks can be identified in the region of 2050–2160 cm^{-1}. We see the spectral shape changes with increase of disilane exposure, indicating that various kinds of hydride are populated and that the type and surface concentration of those hydrides depend on the disilane exposure. We first consider the origin of each peak.

An intense, broad peak can be observed around 2090 cm^{-1}. From its peak position, we assign this peak to Si monohydride (SiH).[19] We interpret that monohydride is populated when hydrogen atoms are released from impinging disilane molecules and then they stick on surface Si dangling bonds. Two peaks are observed at 2112 and 2123 cm^{-1}. According to the assignment by Wu *et al.*,[18] these peaks are indicative of Si dihydride (SiH_2). Additional peaks can be identified at 2134 and 2158 cm^{-1}. Considering its peak position, we attribute the peak at 2134 cm^{-1} to trihydride species (SiH_3).[19] We suppose that upon disilane adsorption the Si—Si bond of the disilane molecule is ruptured to generate two silyl fragments that stick on Si surface dangling bonds. As described below, we tentatively assigned the peak at 2158 cm^{-1} to Si dihydride (SiH_2) in the on-top site of a dimer. We notice that the peaks at 2112, 2123, and 2134 cm^{-1} are slightly shifted to lower frequencies as the disilane exposure increases. This shift would be due to the interaction between adjacent Si—H bonds that increase their surface concentration with increase of disilane exposure. We thus confirm that at room temperature, disilane dissociatively adsorbs onto the Si(100)(2×1) surface to produce all the types of Si hydrides (SiH, SiH_2, and SiH_3). Our main concern in this study is to determine the atomic bonding configurations for those hydride species, which would give us a clue to the elucidation of the mechanism of disilane adsorption on Si(100). In the following, we will discuss the silane adsorption at low and high hydride coverages separately.

We first discuss the adsorption of disilane for low hydride coverage. Figure 3 shows *p*- and *s*-polarized IRAS spectra in the Si-H stretching vibration region that have been collected for 0.5-L disilane exposure. To determine the peak positions more precisely, we have taken the second derivative of the absorption spectra with respect to frequency. The result is shown in the upper portion of Fig. 3. All the types of hydride species show up with monohydride being dominant. It should be noticed that the trihydride component is rather weak as compared to the monohydride and dihydride peaks. And, it seems that the monohydride peak has some spectral components.

Previous studies suggested that at temperatures above 700 K and fractional surface hydrogen coverage less than one monolayer, Si_2H_6 dissociatively adsorbs on Si surface dan-

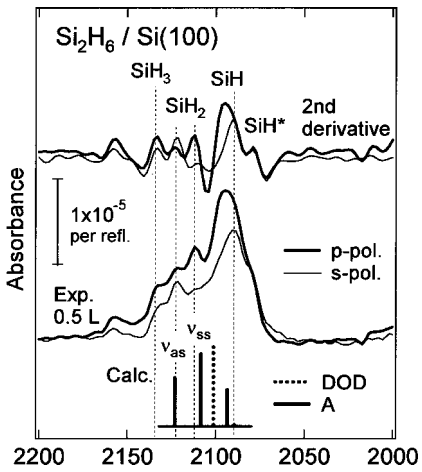

FIG. 3. Si-H stretching vibration spectra of the Si(100) surface exposed to Si_2H_6 at room temperature, compared with cluster calculations. ν_{ss} and ν_{as} indicate the symmetric and antisymmetric vibrations, respectively.

gling bonds as two trihydride (SiH_3) species and then decomposes to surface monohydride (SiH). This is consistent with our observation that the trihydride peak was weak, while the monohydride peak was dominant. However, the adsorption process at low temperature would be different from that at high temperature. At low temperature, disilane might adsorb on the surface without breaking its Si—Si bond. Previous STM studies by Wang *et al*. have demonstrated that at room temperature, disilane dissociates to produce dihydride species ($—SiH_2$) and two monohydride species.[10] The adsorption model they proposed on the basis of their STM images is schematically shown in the upper-left portion of Fig. 4 (labeled A′); in their model, one of the two monohydrides resides on the adjacent dimer row, not on the same dimer row. However, it seems unlikely that at room temperature disilane completely dissociates into monohydride and dihydride species. Furthermore, considering the

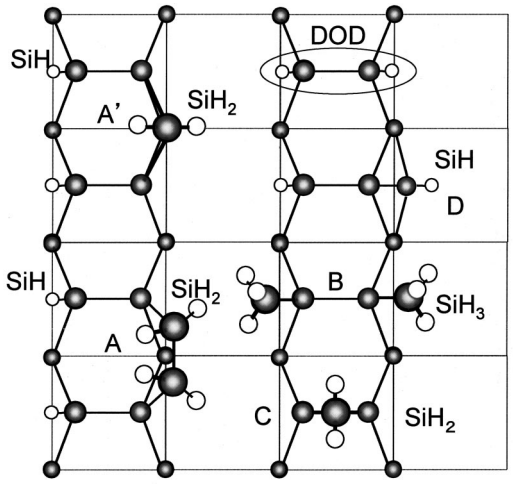

FIG. 4. Bonding geometries of hydride species on the Si(100) $\times(2\times1)$ surface. SiH, SiH2, SiH3, and DOD denote monohydride, dihydride, trihydride, and doubly occupied dimer, respectively.

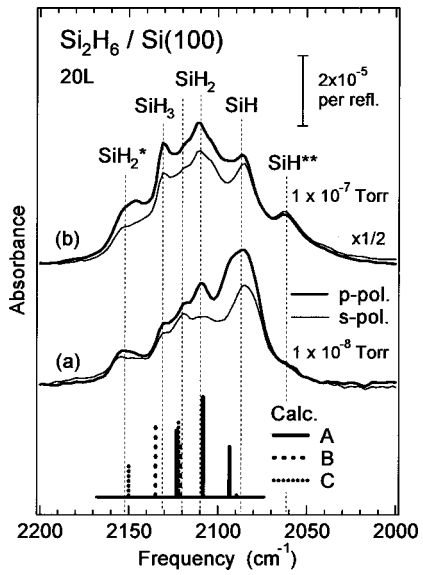

FIG. 5. Si-H stretching vibration spectra of the Si(100) surface exposed to Si_2H_6 at dosing pressures of (a) 10^{-9}–10^{-8} Torr and (b) 10^{-7} Torr, compared with cluster calculations. ν_{ss} and ν_{as} indicate the symmetric and antisymmetric vibrations, respectively.

number of the constituent atoms, we suspect that their model does not explain the disilane adsorption; it would rather be applicable to the adsorption of monosilane, SiH_4. One plausible adsorption structure we here propose is schematically depicted in the lower-left portion of Fig. 4 (labeled A in the figure): Two hydrogen atoms that are released from Si_2H_6, terminate Si surface dangling bonds of two adjacent dimers to produce two monohydrides, and the remaining fragment adsorbs onto the bridge site of the two dimers to produce an *adatom dimer*, $—H_2Si—SiH_2—$. Note that the adatom dimer has two Si dihydrides. We hereafter refer to this adsorption structure as ''A.'' In order to determine which adsorption structure, A or A′, is formed at room temperature, we have carried out a detailed theoretical analysis of the Si-H stretching vibration frequencies that is essential for an unequivocal characterization of the adsorption structure. The results will be presented below. Of course, we cannot exclude the possibility that upon its adsorption, the disilane molecule dissociates to generate two silyl ($—SiH_3$) groups that subsequently decompose to monohydride. In fact, although its intensity was quite low, the trihydride peak showed up, as can be seen in Fig. 3. This indicates that the reaction channel leading to the formation of two SiH_3 is indeed open.

Next we will present the results obtained for high exposures, i.e., high hydride coverage. In Fig. 5(a), we show typical spectra of the surface that was exposed to disilane for 20 L at dosing pressures of 10^{-9}–10^{-8} Torr. The spectral shape is similar to that observed for low exposures except that the dihydride and trihydride peaks are slightly enhanced as compared to the monohydride one. However, the surface dosed with disilane at a higher dosing pressure exhibited quite different spectral features. We plot in Fig. 5(b) typical spectra of the surface that was exposed to disilane for the same exposure (20 L) at the dosing pressure of about

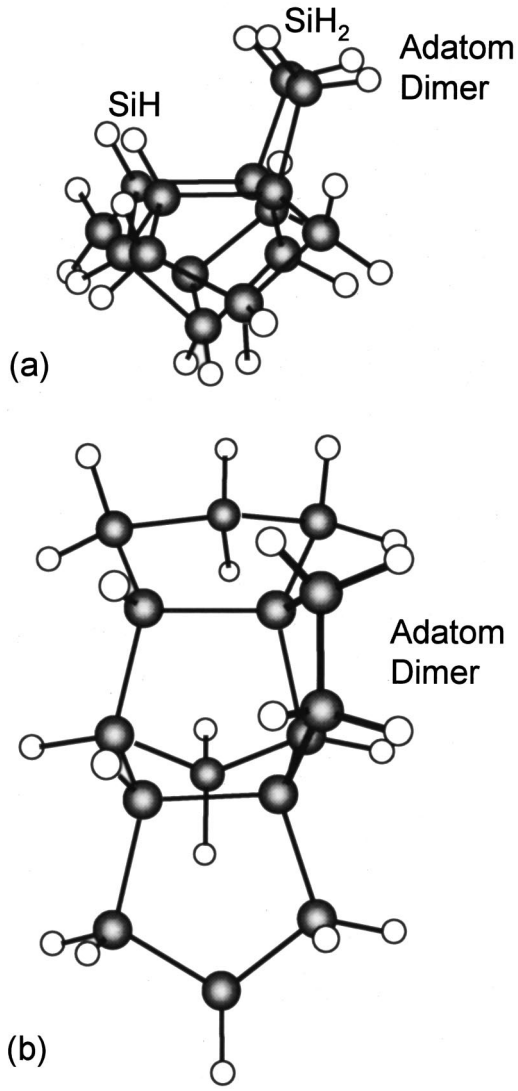

FIG. 6. (a) Side view and (b) top view of bonding geometries of an adatom dimer.

10^{-7} Torr. The spectra of Fig. 5(b) are consistent with the previous results of Wu *et al.*[18] Notice that the dihydride and trihydride components are lager in intensity than the monohydride peak, which is in sharp contrast to the case of low dosing pressure. This difference will be discussed in more detail later.

B. Cluster calculations

In order to determine the adsorption structure precisely, we have carried out a detailed theoretical analysis of the Si-H stretching vibration frequencies. To simulate the silicon surface, we employ a cluster model that contains 13 silicon atoms whose unphysical dangling bonds are terminated by hydrogen, as is depicted in Fig. 6. In electronic structure calculations, we adopt the well established hybrid DFT (B3LYP) with the basis set of the polarized double-zeta Gaussian-type orbitals (6-31G**): Based on Becke's method,[21] the electron many-body energy functional is a mixture of the exact exchange energy and of the exchange correlation energy in the conventional DFT (the local-density approximation and generalized gradient approximation). We first optimize the geometries of surfaces, and then obtain the vibration frequencies of surface hydrogen modes. In calculating these frequencies, we assign artificially heavy mass to the terminating hydrogen atoms so that the motion of terminating atoms is excluded from the surface modes. All the calculations are performed using the GAUSSIAN 98 program.[22] We have introduced the scaling factor of 0.9613 for the 6-31G** basis set; this value is widely used in evaluating vibration frequencies.

TABLE I. A summary of theoretical and experimental frequencies (cm^{-1}) of the structures shown in Fig. 3. The values in parentheses are relative to the frequency of the DOD ν_s SiH mode.

Structure	Mode	Theory	Experiment
A(—H_2Si—SiH_2—)	ν_s SiH_2	2108 (+7)	2112 (+15)
A(—H_2Si—SiH_2—)	ν_a SiH_2	2123 (+22)	2123 (+26)
A(—H_2Si—SiH_2—)	ν SiH	2090 (−11)	(2090) (−7)
		2093 (−8)	
A′(—H_2Si—)	ν_s SiH_2	2100 (−1)	2099[a] (+2)
A′(—H_2Si—)	ν_a SiH_2	2117 (+16)	2115[a] (+18)
A′(—H_2Si—)	ν SiH	2089 (−12)	2093[a] (−4)
		2092 (−9)	
		2123 (+22)	
B(—SiH_3)	ν SiH_3	2134 (+33)	2134 (+37)
		2137 (+36)	
C(—SiH_2—)	ν_s SiH_2	2122 (+21)	2158 (+61)
C(—SiH_2—)	ν_a SiH_2	2150 (+49)	
DOD(═HSi—SiH═)	ν_s SiH	2101	2097[b]
DOD(═HSi—SiH═)	ν_a SiH	2093 (−8)	2087[b] (−10)

[a]From IRAS spectra of SiH_4/Si(100).
[b]From Ref. 19.

Comparison between the experimental and computed frequencies is summarized in Table I. The so-called doubly occupied dimer (DOD), in which a hydrogen atom is attached to each Si atom of a dimer as depicted in the upper-right portion of Fig. 4, is an obvious choice for calibration of the computed frequencies in this spectral region.[14] As seen in Table I, the computed frequencies at 2093 and 2101 cm^{-1} are in good agreement with the observed ones: 2087 and 2097 cm^{-1}.[20]

We here briefly discuss the accuracy of our calculation. The scaling factor mentioned above was determined to reproduce experimental frequencies of a variety of chemical systems. Therefore it is considered to correct the harmonic approximation used in the hybrid-DFT calculations. In the Si-H stretching modes, the anharmonic effect is expected to reduce frequencies by about 30 cm^{-1}, as has been demonstrated by R. Honke *et al.*[23] on their theoretical study on the Si(111): H surface. We understand that the scaling factor is introduced into the calculations so as to take into account this frequency lowering due to the anharmonic effect. We recognize that the B3LYP calculation with the scaling factor induces a deviation of vibration frequency of about ten wave numbers, typically 10–20 cm^{-1}, from the experimental

values.[24] In order to examine the validity of our cluster model, we enlarged the cluster size to confirm that the frequency varies within 10 cm^{-1}. We therefore conclude that our calculations are well converged for the cluster size. In Table I, we compare the calculated frequencies of hydride species for some plausible adsorption structures with the observed ones. In the table, we tabulated relative frequencies ($\Delta\nu$) that are the deviations from the calculated frequency for the DOD symmetric mode. We have assigned the observed hydride peaks by comparing the experimental and theoretical relative frequencies, $\Delta\nu$.

C. Adsorption structure

We discuss the detailed adsorption structure of Si hydride species that form upon disilane adsorption. We first consider the origin of the dihydride peak observed in the spectra of Fig. 3. We see from Table I that a dihydride of the adatom dimer, —SiH_2—SiH_2—, has calculated antisymmetric and symmetric Si-H stretching frequencies (2123 and 2108 cm^{-1}) in good agreement with experimentally observed modes (2123 and 2112 cm^{-1}). The calculated values of $\Delta\nu$ are also consistent with the experimental ones, as can be seen in Table I. We show the calculated frequency and oscillator strength for each vibration mode by solid and dotted bars in Fig. 3. It should be noticed that in the *s*-polarized spectrum, the peak at 2112 cm^{-1} is lower in intensity than the peak at 2123 cm^{-1}. In the *p*-polarized spectrum, on the other hand, the peak at 2112 cm^{-1} is higher in intensity than the peak at 2123 cm^{-1}. As is illustrated in Fig. 6, the adatom dimer protrudes from the surface nearly normal to the surface and the direction of the symmetric vibration of the dihydride is nearly perpendicular to the surface, correspondingly. We can therefore anticipate that the symmetric vibration be suppressed for the *s* polarization, which is consistent with our experimental results. Thus the observed polarization dependence gives further support to our assignment. As is shown in Table I, the calculated frequency of the symmetric vibration mode of the A′-site dihydride is predicted to be 2100 cm^{-1} ($\Delta\nu = -1\ cm^{-1}$) and that of the antisymmetric vibration mode is 2117 cm^{-1} ($\Delta\nu = +16\ cm^{-1}$). In this case, the calculation cannot explain the positions of the experimentally observed doublet structure, 2112 and 2123 cm^{-1}. We thus suggest that upon room-temperature adsorption of Si_2H_6, the adatom dimer, —SiH_2SiH_2—, is populated.

In order to get further support to our assignment, we have measured IR spectra of the surface that was exposed to monosilane, SiH_4. We expected that during SiH_4 adsorption, an isolated dihydride be favorably generated; the monosilane misses two hydrogen atoms to produce a single dihydride fragment, $=SiH_2$. We plot in Fig. 7 typical IRAS spectra in the Si-H stretching vibration region of the surface that was exposed to monosilane (SiH_4) at room temperature. The surface exhibits spectral features quite different from the Si_2H_6-adsorbed surface. Vertical bars shown in the bottom of Fig. 7 show the results of cluster calculation obtained under the assumption that monosilane dissociates to produce DOD and isolated hydride species as illustrated in Fig. 4 (structure A′). Agreement between the calculation and the experiment

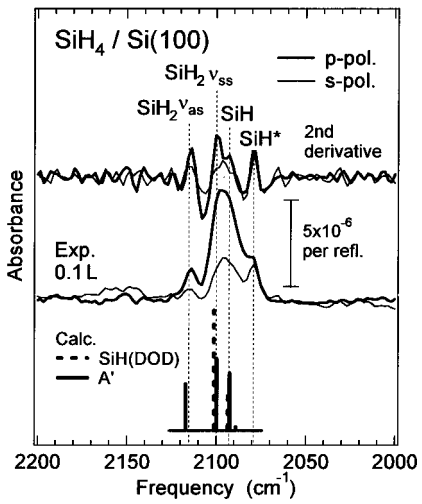

FIG. 7. Si-H stretching vibration spectra of the Si(100) surface exposed to SiH_4 at room temperature, compared with cluster calculations. ν_{ss} and ν_{as} indicate the symmetric and antisymmetric vibrations, respectively.

is fairly good, which indicates that SiH_4 adsorption produces an *isolated* dihydride that bridges two adjacent dimers. Hence we conclude that disilane adsorption produces an adatom dimer in the bridge site between two adjacent dimers.

On the basis of the results of cluster calculations, we will consider the origin of the other hydride peaks. As can be seen in Fig. 3, cluster calculations suggest that the peak at 2090 cm^{-1} contains the DOD component, besides the monohydride component of structure A. The existence of the DOD component is supported by the polarization dependence of the Si-H vibration spectra: As described above, DOD exhibits two peaks at 2087 and 2097 cm^{-1}; the former is due to the antisymmetric vibration and the latter the symmetric vibration.[20] Considering the bonding geometry, we can expect that the symmetric vibration be suppressed for the *s*-polarization condition. Close inspection of Fig. 3 indicates that the absorbance around 2100 cm^{-1} is lower in the *s*-polarized spectrum than in the *p*-polarized spectrum. This suggests that the DOD component is contained in the peak at 2090 cm^{-1}. As described previously, we assigned the peak at 2134 cm^{-1} to a trihydride. The results of cluster calculation confirm our assignment as can be seen in Fig. 5. To explain the peak at 2158 cm^{-1}, we considered a dihydride that resides in the on-top site of a dimer with the dimer bond retained (labeled C in Fig. 4). The calculated symmetric and antisymmetric vibration frequencies of this dihydride are 2122 and 2150 cm^{-1}, respectively, as shown in Fig. 5 and Table I. We therefore tentatively assigned the 2158-cm^{-1} peak to the ''on-top'' dihydride; the symmetric vibration component would be included in the intense dihydride peak at 2123 cm^{-1}. Cluster calculation could not explain the appearance of the SiH* peak at 2079 cm^{-1} by assuming simple bonding geometries. We assumed such a bonding configuration as illustrated in Fig. 4 (labeled D in the figure); a monohydride Si atom is bound to a dimer Si atom as well as two Si atoms on the second layer of the substrate. The computed Si-H stretching frequency for this monohydride species is

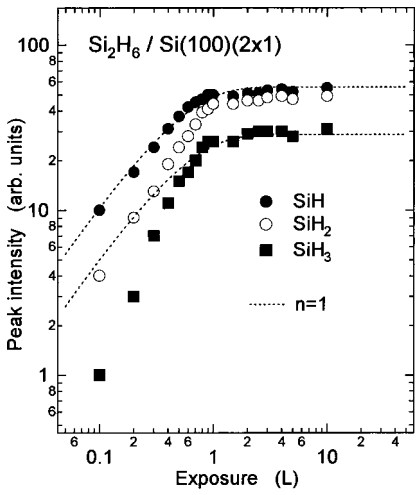

FIG. 8. Relative intensities of the monohydride (2090 cm^{-1}), dihydride (2123 cm^{-1}), and trihydride (2134 cm^{-1}) peaks as a function of disilane exposure. Dotted curves shows the uptake curve predicted from the first-order adsorption kinetics.

2074 cm^{-1}, which is close to the observed frequency, 2079 cm^{-1}. Accordingly, we tentatively assigned the SiH* peak to a *strained* monohydride of adsorption structure D. This peak can be clearly identified for adsorption of SiH_4 as well, as shown in Fig. 7. Considering its bonding configuration, we suspect that SiH* is favorably populated at step sites on the surface. The spectra of Fig. 5(b) exhibit a peak at 2060 cm^{-1}. We speculate the peak, as indicated by SiH** in Fig. 5(b), is also a monohydride species that has a rather complicated bonding configuration. More elaborate investigation would be needed on the origin of these monohydride species.

D. Hydride decomposition

The spectra of Fig. 2 show that at low exposure the intensity of the SiH_3 peak is quite low as compared to that of the SiH peak. This trend can be clearly seen in Fig. 8 where we plot the intensities of the monohydride, dihydride, and trihydride peaks as a function of disilane exposure. Dotted curves shown in Fig. 8 indicate the uptake curve predicted from the first-order adsorption kinetics. We can see than dihydride and trihydride does not exhibit the first-order kinetics, while the formation of monohydride obeys the first-order kinetics; especially, the trihydride peak intensity is quite low at low exposures. We interpret this fact as being due to the decomposition of trihydride species. As previously demonstrated, when disilane adsorbs on the Si surface, the Si—Si bond of the molecule is ruptured to generate two trihydride species, and trihydrides thus generated may further decomposes to monohydride and dihydride species. It should be pointed out that this trihydride decomposition requires unsaturated Si dangling bonds around the trihydride species; otherwise hydrogen atoms released from the trihydride cannot migrate on the surface to produce new Si—H bonds. This requirement will be satisfied when the surface hydride coverage is low. On the surface with low hydride coverage, therefore, trihydrides readily decompose to monohydride or dihydride species. This leads to a reduction in intensity of the trihydride peak. Instead, the monohydride and dihydride peaks would increase their intensities. On the other hand, high hydride coverage reduces the concentration of unsaturated dangling bonds, thereby giving rise to suppression in the reaction rate of trihydride decomposition.

The spectra of Fig. 5 give experimental evidence for the above interpretation. We see from Fig. 5 that the trihydride peak is much higher in intensity on the surface dosed with disilane at a high dosing pressure than on the surface exposed to disilane at a lower dosing pressure. In contrast, the monohydride peak intensity was rather high when the dosing pressure of disilane was low. For low dosing pressure, the impinging rate of disilane molecules on the surface should be low, and correspondingly the time during which the adsorbed trihydride have unsaturated dangling bonds around it, should be long enough for the trihydride to further decompose to monohydride or dihydride. This will facilitate the decomposition of trihydride, leading to an enhancement of the monohydride peak intensity. For high dosing pressure, on the other hand, the impinging rate should be high and therefore the density of unsaturated dangling bonds rapidly decreases with increase of disilane exposure. In this case, the adsorbed trihydride will be hard to migrate and decompose, and therefore retains unchanged. This results in an enhanced intensity for trihydride and correspondingly a reduced intensity for monohydride.

It should be noticed that even at low hydride coverage the SiH* peak showed up. We interpret that SiH* was populated via the decomposition of trihydride species. One possible reaction path leading to the SiH* formation would be as follows: the decomposition of trihydride produces two hydrogen atoms and a Si-H fragment: $—SiH_3 \rightarrow H + H + SiH$. Hydrogen atoms released from the trihydride likely migrate on the surface with dangling bonds to form monohydride species such as DOD. Note that DOD is energetically quite stable. We suppose that the remaining SiH fragment also may migrate on the surface. When it is trapped at defects sites such as vacancies and steps, then SiH* would be generated. We believe that SiH* is energetically rather stable. Therefore SiH* does not further migrate on the surface or decompose.

The main points of the above argument are that disilane adsorption produces various kinds of hydrides on the surface and that some of those surface hydride species may be energetically unstable and therefore readily decompose. As described above, we suggest that trihydride species is such a hydride species that decomposes to lower hydride species even at room temperature. On the other hand, the adatom dimer, DOD and monohydride SiH* are considered to be relatively stable against decomposition and therefore remain unchanged for a long term. However, it should be pointed out that hydride decomposition is affected by the surface hydride coverage.

IV. CONCLUSIONS

We have investigated the adsorption of disilane on Si(100) (2×1) using infrared absorption spectroscopy. We demonstrated that during room-temperature adsorption, disi-

lane dissociatively adsorbs onto surface Si dangling bonds to produce mono-, di-, and trihydride species, and that the hydride distribution depends on the surface hydride coverage. From comparison of IR data with hybrid density-functional cluster calculation, we suggested the formation of an adatom dimer, $—H_2Si—SiH_2—$ that bridges two adjacent dimmers. We showed that at low hydride coverage, a trihydride ($—SiH_3$) decomposes to monohydrides, while at high hydride coverage the trihydride decomposition is quenched. The present results also suggested that the dosing pressure of the source gas has a significant effect on the disilane adsorption kinetics on Si surfaces.

ACKNOWLEDGMENT

Part of this work was supported by a Grand-in-Aid for Basic Scientific Research (Grant No. 11304018) from the Ministry of Education, Science, Sports and Culture of Japan.

*Corresponding author. FAX: +81-22-217-5503; electronic mail: niwano@riec.tohoku.ac.jp

[1] D. Lubben, R. Tsu, T. R. Bramblett, and J. E. Greene, J. Vac. Sci. Technol. A **9**, 3003 (1991).
[2] T. R. Bramblett, Q. Lu, T. Karasawa, M.-A. Hasan, S. K. Jo, and J. E. Greene, J. Appl. Phys. **76**, 1884 (1994).
[3] T. R. Bramblett, Q. Lu, N.-E. Lee, N. Taylor, M.-A. Hasan, and J. E. Greene, J. Appl. Phys. **77**, 1504 (1995).
[4] S. M. Gates, Surf. Sci. **197**, 307 (1988).
[5] M. Suemitsu, H. Nakazawa, and N. Miyamoto, Surf. Sci. **357/358**, 555 (1996).
[6] R. Imbihl, J. E. Demuth, S. M. Gates, and B. A. Scott, Phys. Rev. B **39**, 5222 (1989).
[7] Y. Suda, D. Lubben, T. Motooka, and J. E. Greene, J. Vac. Sci. Technol. A **8**, 61 (1990).
[8] A. C. Dillon, M. B. Robinson, and S. M. George, Surf. Sci. Lett. **295**, L998 (1993).
[9] X. F. Hu, Z. Xu, D. Lim, M. C. Downer, P. S. Parkinson, B. Gong, G. Hess, and J. G. Ekerdt, Appl. Phys. Lett. **71**, 1376 (1997).
[10] Yajun Wang, M. J. Bronikowski, and R. J. Hamers, Surf. Sci. **311**, 64 (1994).
[11] N. J. Harrick, *Internal Reflection Spectroscopy* (Wiley, New York, 1967), second printing (Harrick, Ossining, 1979).
[12] Y. J. Chabal, Surf. Sci. Rep. **8**, 211 (1988).
[13] F. M. Mirabella, Jr., and N. J. Harrick, *Internal Reflection Spectroscopy: Review and Supplement* (Harrick, Ossining, 1985).
[14] M. K. Weldon, B. B. Stefanov, K. Raghavachari, and Y. J. Chabal, Phys. Rev. Lett. **79**, 2851 (1997).
[15] M. Niwano, M. Terashi, M. Shinohara, and Daisei Shoji, Surf. Sci. **401**, 364 (1998).
[16] M. Terashi, J. Kuge, M. Shinohara, D. Shoji, and M. Niwano, Appl. Surf. Sci. **130–132**, 260 (1998).
[17] M. Niwano, M. Terashi, and J. Kuge, Surf. Sci. **420**, 6 (1999).
[18] Y. M. Wu, J. Baker, P. Hamilton, and R. M. Nix, Surf. Sci. **295**, 133 (1993).
[19] Y. J. Chabal and K. Raghavachari, Phys. Rev. Lett. **53**, 282 (1984).
[20] Y. J. Chabal, Surf. Sci. **168**, 594 (1986).
[21] A. D. Becke, J. Chem. Phys. **98**, 5648 (1993); **88**, 1053 (1988); C. Lee, W. Yang, and R. G. Parr, Phys. Rev. B **37**, 785 (1988).
[22] M. J. Frisch, G. W. Trucks, H. B. Schlegel, G. E. Scuseria, M. A. Robb, J. R. Cheeseman, V. G. Zakrzewski, J. A. Montgomery, Jr., R. E. Stratmann, J. C. Burant, S. Dapprich, J. M. Millam, A. D. Daniels, K. N. Kudin, M. C. Strain, O. Farkas, J. Tomasi, V. Barone, M. Cossi, R. Cammi, B. Mennucci, C. Pomelli, C. Adamo, S. Clifford, J. Ochterski, G. A. Petersson, P. Y. Ayala, Q. Cui, K. Morokuma, D. K. Malick, A. D. Rabuck, K. Raghavachari, J. B. Foresman, J. Cioslowski, J. V. Ortiz, A. G. Baboul, B. B. Stefanov, G. Liu, A. Liashenko, P. Piskorz, I. Komaromi, R. Gomperts, R. L. Martin, D. J. Fox, T. Keith, M. A. Al-Laham, C. Y. Peng, A. Nanayakkara, C. Gonzalez, M. Challacombe, P. M. W. Gill, B. Johnson, W. Chen, M. W. Wong, J. L. Andres, C. Gonzalez, M. Head-Gordon, E. S. Replogle, and J. A. Pople, GAUSSIAN 98, Revision A.7 (Gaussian, Inc., Pittsburgh, PA, 1998).
[23] R. Honke, P. Jacob, Y. J. Chabal, A. Dvořák, S. Tausendpfund, W. Stigler, P. Pavone, A. P. Mayer, and U. Schröder, Phys. Rev. B **59**, 10 996 (1999).
[24] M. W. Wong, Chem. Phys. Lett. **256**, 391 (1996).